analytical chemistry

Article

pubs.acs.org/ac

Smart DNA Machine for Carcinoembryonic Antigen Detection by Exonuclease III-Assisted Target Recycling and DNA Walker Cascade Amplification

Meng-Qi He,[†] Kun Wang,[†] Wen-Jing Wang, Yong-Liang Yu,* and Jian-Hua Wang*

Research Center for Analytical Sciences, Department of Chemistry, College of Sciences, Northeastern University, Box 332, Shenyang 110819, China

Supporting Information

ABSTRACT: A synthetic DNA machine performs quasi-mechanical movements in response to external intervention, suggesting the promise of constructing sensitive and specific biosensors. Herein, a smart DNA walker biosensor for label-free detection of carcinoembryonic antigen (CEA) is developed for the first time by a novel cascade amplification strategy of exonuclease (Exo) III-assisted target recycling amplification (ERA) and DNA walker. ERA as the first stage of amplification generates the walker DNA, while the autonomous traveling of the walker DNA on the substrate-modified silica microspheres as the second stage of amplification produces an ultrasensitive fluorescent signal with the help of *N*-methylmesoporphyrin IX (NMM). The DNA machine as a biosensor could be applied for transducing and quantifying signals from isothermal molecular amplifications, avoiding the complicated reporter elements and thermal cycling. The present biosensor achieves a detection limit of 1.2 pg·mL^{-1} within a linear range of 10 pg·mL^{-1} to 100 ng·mL^{-1} for CEA, along with a favorable specificity. The practical applicability of the biosensor is demonstrated by the detection of CEA in human serum with satisfactory results; thus, it shows great potential in clinical diagnosis.

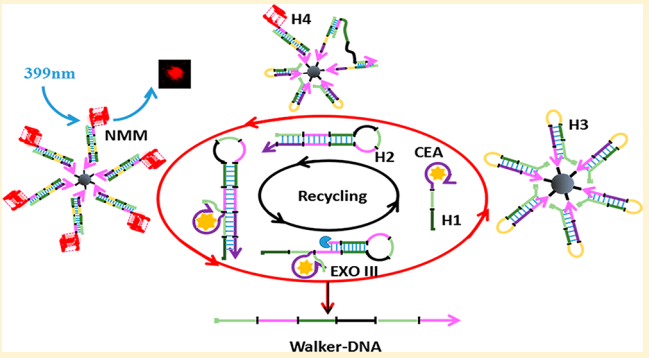

Nucleic acids, by virtue of the programmable, precise, high-throughput, and automated design, serve as an excellent building block for DNA biosensors.[1,2] In this context, various DNA biosensors based on electrochemistry,[3−5] photoelectrochemistry,[6,7] electrochemiluminescence,[8,9] fluorescence,[10−12] and chemiluminescence[13,14] are developed for the detection of biomolecules in clinical research. Due to the low concentration of target biomolecules in the early stages of disease, it is highly desirable to improve the sensitivity for the detection of disease-related biomolecules.[15,16] Thus, a series of amplification strategies, e.g., Exo III-assisted target recycling amplification (ERA),[17,18] hybridization chain reaction (HCR),[19,20] polymerase chain reaction (PCR),[21,22] rolling circle amplification (RCA),[23,24] and strand displacement amplification (SDA),[25,26] are alternatives to improve the sensitivity of DNA biosensors. Among these strategies, ERA is widely employed for the detection of biomolecules due to the nonspecific recognition of Exo III.[27] In fact, Exo III is able to catalyze the stepwise digestion of mononucleotides from the recessed 3′ terminus or the blunt of double-stranded DNA (dsDNA) to recycle target. It shows a lower activity on single-stranded DNA (ssDNA) or dsDNA with a protruding 3′ terminus.[28,29] Furthermore, ERA as a powerful isothermal nucleic acid amplification technique helps to accumulate considerable copies.

DNA is known as an architectural scaffold of DNA biosensors and exhibits an immense promise for applications in the field of nanotechnology.[30] DNA nanotechnology takes the principle of complementary base pairing to create static structures that further perform procedural assembly operations by DNA machines, e.g., DNA walkers and DNA tweezers.[31,32] The introduction of DNA walker into a DNA biosensor throws a new light on the improvement of detection sensitivity. DNA walker has been previously demonstrated to be feasible to conduct the amplification and transduction of signal at the terminus of DNA amplification systems.[33] However, traditional DNA walkers are a class of DNA nanomachines that move along a one-dimensional (1-D) track or a two-dimensional (2-D) surface.[34,35] In contrast, three-dimensional (3-D) tracks possess powerful DNA enrichment capacity due to the large specific surface area of nanoparticles,[36] and thus, 3-D tracks have better amplification performance than 1-D or 2-D tracks. In addition, label-free biosensors provide further promise without the labeling of electrochemical,[3] colorimetric,[37] or fluorescent[38] reporter elements for measurements. The most important aspects are to preserve the integrity of the

Received: May 31, 2017
Accepted: August 14, 2017
Published: August 14, 2017

DOI: 10.1021/acs.analchem.7b02073
Anal. Chem. 2017, 89, 9292−9298

identification element and the capability of identifying the target.[39]

Given the specificity for the detection of biomolecules, the use of aptamer provides an ideal alternative to improve the specificity of DNA walker biosensors. Aptamers, as a type of single-stranded RNA or DNA with a certain sequence, have been discovered and designed with the systematic evolution of ligands by exponential enrichment (SELEX).[40,41] Furthermore, an aptamer is characterized by high affinity and specificity, low cost, high stability, and small size with respect to an antibody. Currently, various aptamer-based biosensors (aptasensors) are exploited for the detection of biomolecules, e.g., an aptazyme−gold nanoparticle sensor,[4] a proximity binding and metal ion-dependent DNAzyme cyclic amplification integrated aptasensor,[42] and tuning the aggregation/disaggregation behavior of graphene quantum dots by a structure-switching aptamer.[43]

DNA walkers have been frequently performed and constructed but rarely found applications in real biosensing.[44] Incorporating DNA nanotechnology into biosensors with the cascade amplification strategy of ERA and DNA walker remains in its infancy. The introduction of the cascade amplification strategy would extremely improve the detection sensitivity of the biosensor and open up a new approach for a DNA walker to merge with biosensor. In the present work, a novel DNA machine is designed for highly sensitive and specific detection of carcinoembryonic antigen (CEA) based on a cascade amplification strategy of ERA and DNA walker. First, the specific aptamer−target recognition moiety of the DNA machine produces a new single-stranded product output, i.e., walker DNA, with the aid of a novel ERA strategy. Then, the walker DNA is propelled by hybridization with immobilized hairpin DNA reporter 1 (H3) to walk on the surface of a microsphere, and during this process a series of ssDNAs generated are hybridized with hairpin DNA reporter 2 (H4) to form G-quadruplex species which could further produce an ultrasensitive fluorescent signal output with the help of *N*-methylmesoporphyrin IX (NMM).[45] Surprisingly, a single walker DNA can catalyze the autonomous assembly of H3 in the free-running progress of the DNA walker and generate more than one signal molecule, giving rise to the prominent fluorescence improvement. CEA has been demonstrated as a broad spectrum tumor biomarker for lung cancer, breast cancer, and colon cancer.[46,47] Hence, the present biosensor holds a great potential for clinical diagnosis by virtue of its high sensitivity and selectivity.

EXPERIMENTAL SECTION

Chemicals and Materials. All the oligonucleotides are synthesized and purified by Sangon Biotechnology Co., Ltd. (Shanghai, China), and their sequences are listed in Table S1. The DNA stock solutions are prepared in Tris/Mg/K buffer containing 10 mM Tris−HCl, 4 mM $MgCl_2$, and 15 mM KCl at pH 8.0, and stored at −20 °C. The oligonucleotides are determined by measuring the UV−vis absorption at 260 nm. CEA is purchased from Linc-Bio Science Co., Ltd. (Shanghai, China). Exo III with a concentration of 200 U μL^{-1} in a buffer containing 50 mM Tris−HCl, 5 mM $MgCl_2$, and 1 mM DTT at pH 8.0, Gel-Red and loading buffer are obtained from TaKaRa Biotechnology Co., Ltd. (Dalian, China). *N*-Methylmesoporphyrin IX, purchased from Porphyrin Products (Logan, UT, U.S.A.), is prepared in dimethyl sulfoxide (DMSO). Carboxyl-modified silica microspheres with a size of 1 μm are achieved from DAE Scientific Co., Ltd. (Tianjin, China). 2-(*N*-Morpholino)ethanesulfonic acid (MES) is the product of Sigma-Aldrich (Shanghai, China), and *N*-(3-(dimethylamino)-propyl)-*N*-ethylcarbodiimide (EDC) is obtained from Aladin (Shanghai, China). Other chemicals used are at least of analytical reagent grade and obtained from Aladin (Shanghai, China) unless otherwise specified. A Milli-Q ultrahigh-purity water of 18 MΩ cm is used throughout the experiments.

Apparatus. UV−vis absorption spectra are recorded on a U-3900 UV−vis spectrophotometer (Hitachi, Japan). The fluorescence spectra are recorded on an F-7000 fluorescence spectrophotometer (Hitachi High Technologies, Japan) at room temperature by irradiating NMM at an excitation wavelength of 399 nm. An FV1200 confocal fluorescence microscope is used to conduct fluorescence imaging (Olympus, Japan). The image of gel electrophoresis is scanned by the gel imaging analysis system (Shanghai Furi Science & Technology Co., Ltd.).

Preparation of Carboxylated Silica Microspheres Modified with H3. The detailed fabrication procedure of carboxylated silica microspheres modified with H3 is described briefly herein: NH_2-terminated H3 is coupled to carboxylated silica microspheres by a single-step carbodiimide reaction. An amount of 500 μL of 25 mg·mL^{-1} silica microspheres is washed with 500 μL of 100 mM MES buffer at pH 4.8 for three times, and subsequently resuspended in 500 μL of the same buffer. An amount of 500 μL of 100 mM MES buffer containing 10 mg·mL^{-1} EDC and 10 μM H3 is prepared. This EDC/oligonucleotide solution is added to the silica microspheres solution and incubated on a water-bathing vibrator at 25 °C and 250 rpm for overnight. After incubation, the microspheres are washed with 500 μL of MES buffer for three times, and finally resuspended in 500 μL of the same buffer. The as-prepared H3-functionalized silica microsphere is presented by the surface coverage and the coupling efficiency of surface −COOH with the $-NH_2$ of H3, as detailed in the Supporting Information. According to the immobilization efficiency measured by the fluorescence of FAM (5-carboxy fluorescein) (Figure S1), the concentration of H3 on the silica microspheres surface is calculated to be 5.2 μM. The functionalized microspheres are stored at 4 °C for further use. Scanning electron microscopy (SEM) and transmission electron microscopy (TEM) images of the silica microspheres are shown in Figure S2.

Exo III-Assisted Target Recycling Reaction. First, the solutions of hairpin DNA probe (H1), hairpin DNA reporter (H2), H3, and H4 are heated to 90 °C for 5 min, and then slowly cooled to room temperature to form a stable structure. The analytical procedure of the present DNA biosensor is briefly described in the following: Exo III-assisted target recycling reaction is conducted in 45 μL of homogeneous solution containing 1.0 μM H1, 2.0 μM H2, and 20 U of Exo III. After the addition of 5.0 μL of CEA solution with various concentrations, the mixture is allowed to react for 50 min at 37 °C in an incubator. Finally, 50 μL of the above solution is heated to 65 °C for 5 min to stop the enzyme reaction.

Free-Running Process of DNA Walker and Fluorescence Monitoring. An amount of 50 μL of the above solution is mixed with 260 nM H3 and 500 nM H4 in TNaK buffer containing 20 mM Tris, 140 mM NaCl, and 5 mM KCl at pH 7.5 and, subsequently, incubated at room temperature for 210 min. The H3/H4 complex is obtained during the free-running process of the DNA walker. The mixture is rinsed with Tris/Mg/K buffer to remove the excessive H4. Afterward, 500 μL of

DOI: 10.1021/acs.analchem.7b02073
Anal. Chem. 2017, 89, 9292−9298

Scheme 1. Illustration for the Principle of the DNA Machine for the Detection of CEA Based on the ERA and DNA Walker Cascade Amplification Strategy[a]

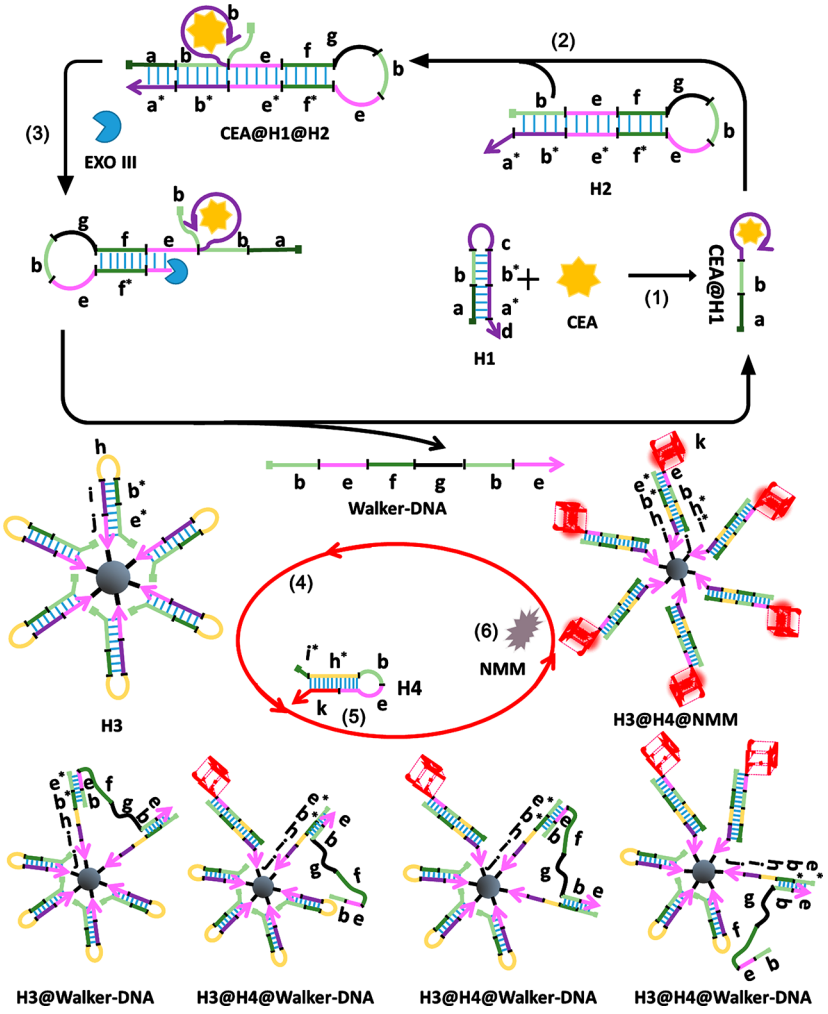

[a]a–k represent DNA sequences, as listed in Table S1; reactions 1–6 represent the free-running process of the DNA machine, as detailed in the Principle of the Cascade Amplification Strategy section.

the reaction solution containing H3/H4 complex and 2 μM NMM is incubated at room temperature for 30 min. Finally, the above solution is thoroughly rinsed with Tris/Mg/K buffer to remove the excessive NMM. The fluorescence is detected at $\lambda_{ex}/\lambda_{em}$ = 399/610 nm.

Validation of the Amplification Strategy by Gel Electrophoresis. Nondenaturing polyacrylamide gel electrophoresis (PAGE) is used to further confirm and characterize the novel DNA machine based on a cascade amplification strategy of ERA and DNA walker. In the PAGE assay, each sample is prepared with TNaK buffer, and the concentration of each DNA strand is 1 μM. A 15% polyacrylamide gel is prepared with 1× TBE buffer (89 mM Tris, 89 mM boric acid, and 2 mM EDTA) at pH 8.3. Am amount of 10 μL of each sample is mixed with 1.5 μL of Gel-Red and 1 μL of loading buffer and loaded into the gel. The gel is operated at 100 V for 3 h and photographed under UV light by a gel imaging analysis system.

Real Serum Samples. Human serum samples are obtained from The First Affiliated Hospital of Dalian Medical University (Dalian, China). The human serum sample is analyzed by following the same procedure as that for CEA detection.

RESULTS AND DISCUSSION

Principle of the Cascade Amplification Strategy. On the basis of the ERA and DNA walker, a smart DNA machine is developed for label-free detection of CEA for the first time. ERA could generate a trigger for activating the walker DNA to walk on the surfaces of H3-coated microspheres, which makes the G-quadruplex bind to the microsphere's surface. When NMM is bound to G-quadruplex, the microspheres are lit up by the NMM/G-quadruplex composites due to the enhanced fluorescence of NMM. The cascade amplification strategy affords a simple, isothermal, and ultrasensitive method for biomolecules detection. The working principle of the DNA machine for the detection of CEA based on ERA and DNA walker cascade amplification strategy is shown in Scheme 1. The sequences of H1 and H2 are rationally and carefully designed to kinetically block any spontaneous interaction between each other in the absence of CEA. Furthermore, both H1 and H2 could self-hybridize into a stem–loop structure with an Exo III resistant 3′ overhanging terminus. Thus, Exo III hardly exhibits any activity on H1 and H2 in the absence of CEA. On the contrary, when the target CEA is introduced to the mixture of H1, H2, and Exo III, it could specifically

DOI: 10.1021/acs.analchem.7b02073
Anal. Chem. 2017, 89, 9292–9298

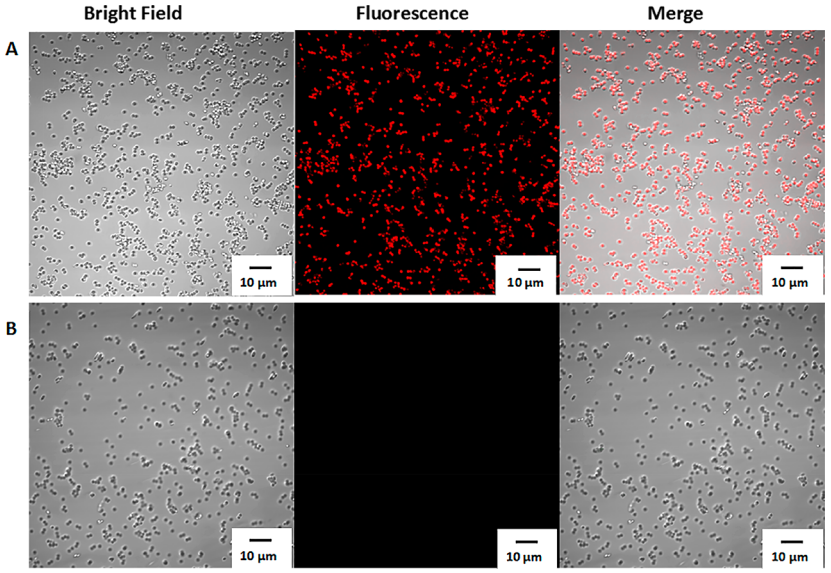

Figure 1. Confocal microscopy images of microspheres after incubation with (A) and without (B) 5 ng·mL^{-1} CEA for 210 min, observed at λ_{ex} 405 nm.

combine with its aptamer region in H1 (c, b*, a*, d), resulting in a conformational change of H1 from the stem−loop structure to the CEA@H1 complex structure and the exposure of the occluded domain a and domain b in the stem regions (reaction 1 in Scheme 1). In this case, the exposed domain a and domain b could hybridize with H2 from its 3′-protruding terminus to form a blunt 3′-terminus (reaction 2), whereupon Exo III catalyzes the stepwise removal of mononucleotides from the protruding domain a* in H2, leading to the release of the CEA@H1 complex along with the ultimate generation of the walker DNA (reaction 3). Importantly, the released CEA@H1 complex could bind another H2 and restart a new cycle. At the same time, the originally caged walker DNA in the rigid stem of H2 is thereby transformed into a flexible walker DNA. A single target CEA is able to generate the abundance of walker DNA, leading to a distinct increase in the fluorescent signal. Furthermore, the amount of the walker DNA traversing on the silica microsphere surface correlates positively with the concentration of the target CEA.

In the free-running process of DNA walker, walker DNA is able to interact with a toehold e* on surface-bound H3 and open H3 via toehold-mediated strand exchange to form H3@walker DNA (reaction 4). The new exposed toehold i on H3 would hybridize to a toehold i* on H4 and trigger a strand exchange reaction, ultimately forming an H3@H4@walker DNA tripartite complex (reaction 5). As the H3@H4 complex tends to form a thermodynamically favorable configuration, walker DNA would be released and participate in the subsequent reaction cycles. In the H3@H4 complex, domain k of hairpin H4 forms a G-quadruplex structure that could bind with the small-molecule dye NMM (reaction 6). This G-quadruplex structure drastically increases the fluorescence signal of NMM.[48] It is noteworthy that the use of microsphere as a carrier brings obvious advantages with respect to that of an individual indicator for the detection of biomolecules, e.g., the increase of brightness and the elimination of interferences.[49] It is because that large specific surface area of the microsphere brings abundant binding sites for an individual indicator to enhance brightness in response to a single walker DNA-binding event. Meanwhile, microsphere-based separation could remove the excess H4 to reduce the background signals of G-rich sequences (GGGTAGGGCGGGTTGGG) in the free-running process of the DNA walker. Although silica microspheres have the ability for protein adsorption, the present DNA walker biosensor could be ingeniously divided into two parts, including an ERA part and a DNA walker amplification part. Given the specificity for the detection of CEA, the use of aptamer in the first part provides an ideal alternative to improve the specificity of the DNA walker biosensor. The product walker DNA in the first part could be used as an initiator to trigger a recycling in the DNA walker amplification part to enhance the reaction signals. Furthermore, silica microspheres are added in the second part. Therefore, the reaction signals of the DNA machine are related to the product directly and independent of the adsorption capacity of the silica microspheres.

Feasibility of the Cascade Amplification Strategy. The present DNA machine is simple but ingenious in design. It is a longer single-stranded oligonucleotide containing two same catalytic domains (b and e) separated by a linear and nonhybridizing spacer sequence (f and g). It could undergo the multiple cycles of surface-bound catalysis until the microspheres light up. Microscopy experiments further reveal that DNA walker is able to travel between two microspheres with a 3-D track when microspheres are in close contact with each other. Figure 1 shows confocal microscopy images of the microsphere treated with NMM at bright field with an excitation wavelength of 405 nm. In the presence of CEA, the phase contrast images of microspheres clearly show the dispersion of red emission inside the solution along with clear zones of the microsphere surface (Figure 1A). In the absence of CEA, however, the phase contrast images of microspheres exhibit very weak fluorescence (Figure 1B). In addition, a series of control experiments are carried out to further test the fluorescence amplification effect of the biosensor based on the designed ERA and DNA walker cascade in the presence/absence of CEA and with/without Exo III. As depicted in Figure 2, in only the presence of H3 and H4, the fluorescence intensity of NMM is very weak (curve a), suggesting the weak affinity between H3 and H4 without CEA and Exo III. In the absence of target with the addition of H1, H2, H3, H4, and Exo

DOI: 10.1021/acs.analchem.7b02073
Anal. Chem. 2017, 89, 9292−9298

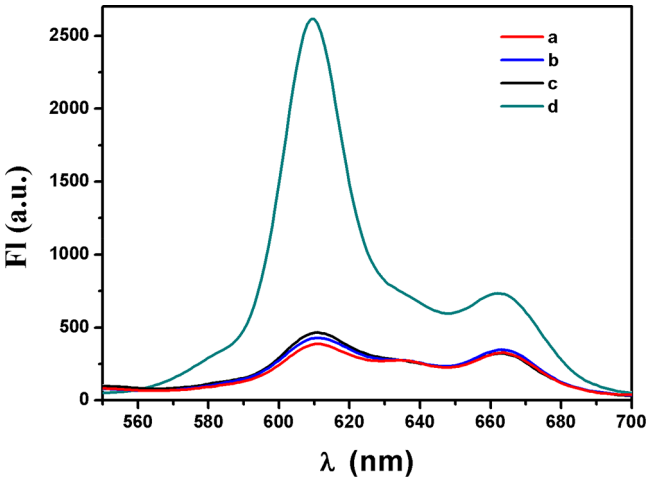

Figure 2. Fluorescence responses of the biosensor toward the reaction mixture of NMM, H3, and H4 (a); NMM, H1, H2, H3, H4, and 20 U of Exo III (b); NMM, H1, H2, H3, H4, and 5 ng·mL^{-1} CEA (c); NMM, H1, H2, H3, H4, 5 ng·mL^{-1} CEA, and 20 U of Exo III (d).

III (20 U), an insignificant fluorescence response is obtained (curve b), which is attributed to the ultralow background reactivity between H3 and H4 as well as the ultralow cleavage activity of Exo III toward the designed H1 and H2 without CEA. Moreover, in the presence of H1, H2, H3, H4, and 5 ng·mL^{-1} CEA without the addition of Exo III (curve c), no obvious change in fluorescence is observed with respect to curve b and curve a, indicating that the Exo III-assisted cyclic cleavage of H2 could be only performed in the presence of both CEA and Exo III. As expected, strong and obvious fluorescence intensity is obtained in the presence of both 5 ng·mL^{-1} CEA and 20 U of Exo III (curve d). This signal increase is ascribed to the microspheres being lit up by the DNA walker, which is generated from the Exo III-assisted cyclic cleavage of H2 and traverses robustly on the surface of the microspheres due to its higher affinity toward H3. Typical progress curve and gel electrophoresis are also utilized to further verify the feasibility of the designed DNA machine for highly sensitive and specific detection of CEA based on a cascade amplification strategy of ERA and DNA walker. The progress curve shows the time-dependent increase in the overall fluorescence intensity (Figure S3A). The gel electrophoresis illustrates the generation of a new DNA strand and H3@H4 complex (Figure S3B).

Optimizations. In order to obtain the best analytical performance, the corresponding experimental conditions are further optimized. The fluorescence response of the present biosensor toward 5 ng·mL^{-1} CEA increases with the amount of Exo III, which almost reaches a plateau at a concentration of 20 U (Figure S4A). Afterward, the fluorescence intensities remain almost constant with further increase of the Exo III amount. Thus, for further experiments the amount of Exo III is chosen as 20 U. The digestion time of the present biosensor for CEA detection is also investigated (Figure S4B). It is found that the fluorescence intensity increases continually with the digestion time from 0 to 80 min and almost reaches a saturation value at 50 min. The optimal reaction time is thus chosen at 50 min. The effect of the reaction time of H3 and H4 on the fluorescence response is shown in Figure S4C. Taking efficiency and sensitivity into consideration, the reaction time is set at 210 min.

Analytical Performance of the Biosensor. Under the optimized conditions, the analytical performance of the present biosensor is investigated by using various concentrations of CEA. As shown in Figure 3A, the fluorescence intensity steadily increases with the concentration of CEA from 0 to 100 ng·mL^{-1}, suggesting that the DNA machine for the fluorescence signal readout is highly dependent on the concentration of CEA. Figure 3B shows a calibration curve by plotting the fluorescence intensity versus the concentration of the target CEA. It shows a favorable linear relationship between the fluorescence intensity and the logarithm of the target CEA concentration within a range of 10 pg·mL^{-1} to 100 ng·mL^{-1}. The linear regression equation is obtained as F (a.u.) = 767 lg[C_{CEA} (ng·mL^{-1})] + 2027 with a correlation coefficient of 0.998. Additionally, the detection limit of the present biosensor for CEA is estimated to be as low as 1.2 pg·mL^{-1} at a signal-to-noise ratio of 3, which is superior to those of the previously reported biosensors based on the amplification strategies of the surface-enhanced fluorescence (3 pg·mL^{-1}), target-induced DNA assembly and cyclic DNA cleavage (48 pg·mL^{-1}), and enzyme-catalyzed generation of numerous signal quencher (1.38 pg·mL^{-1}). The detailed comparisons of analytical performance of the present biosensor with those of other methods based on various amplification strategies for CEA assay are listed in Table S2. These results indirectly reveal the high amplification efficiency of the ERA and DNA walker cascade.

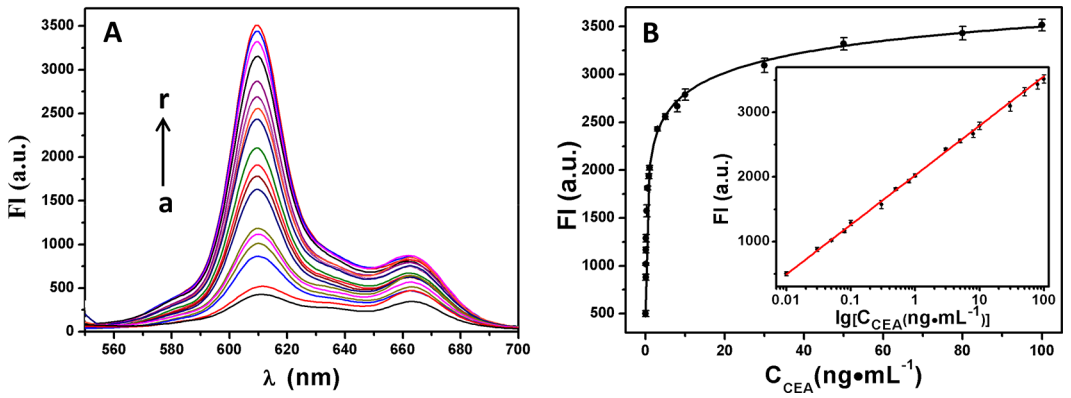

Figure 3. (A) Fluorescence responses of the present biosensor to different concentrations of CEA (from a to r: 0, 0.01, 0.03, 0.05, 0.08, 0.1, 0.3, 0.5, 0.8, 1.0, 3.0, 5.0, 8.0, 10, 30, 50, 80, 100 ng·mL^{-1}). (B) Variation of the peak fluorescence intensity as a function of CEA concentration. Inset: the linear relationship of the peak fluorescence intensity vs the logarithm of CEA concentration.

DOI: 10.1021/acs.analchem.7b02073
Anal. Chem. 2017, 89, 9292−9298

Selectivity of the Biosensor and Its Application in Real Sample Analysis. The selectivity of the proposed fluorescence biosensor is further investigated by using three kinds of protein biomarkers, including α-fetoprotein (AFP), thrombin, and immunoglobulin G (IgG). A series of control experiments are performed by assaying AFP, thrombin, and IgG instead of CEA, respectively, at the same optimal experimental conditions. Figure 4 displays the typical fluorescence peak

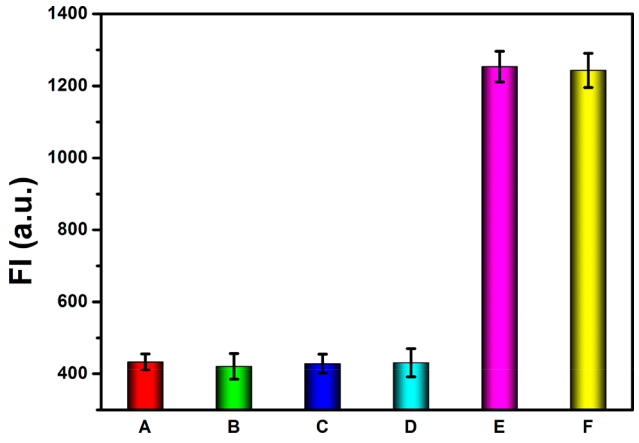

Figure 4. Selectivity test for the present biosensor for CEA assay: (A) blank; (B) 100 pg·mL^{-1} AFP; (C) 100 pg·mL^{-1} thrombin; (D) 100 pg·mL^{-1} IgG; (E) 100 pg·mL^{-1} CEA; (F) 100 pg·mL^{-1} CEA in the presence of 100 pg·mL^{-1} AFP, 100 pg·mL^{-1} thrombin, and 100 pg·mL^{-1} IgG.

responding to 100 pg·mL^{-1} of three different protein biomarkers and the background. It is obvious that the fluorescence response of CEA is much stronger than those of AFP, thrombin, and IgG. Moreover, the addition of AFP, thrombin, or IgG into the target CEA causes virtually no obvious variation compared with the target CEA alone. These observations demonstrate that the designed biosensor could effectively discriminate CEA from other protein biomarkers and display an excellent selectivity for CEA assay.

For the purpose of demonstrating the practical applications and analytical reliability of the designed biosensor, CEA in real human serum samples is assayed as outlined above. Subsequently, different concentrations of CEA are spiked into the serum samples and detected by the same procedure. Table 1 demonstrates favorable spiking recoveries for CEA at various concentration levels. These results clearly indicate the favorable accuracy of the designed biosensor for the detection of CEA in real biological samples.

CONCLUSIONS

In summary, a smart DNA machine is proposed for label-free detection of CEA by a novel cascade amplification strategy of ERA and DNA walker. This DNA machine as a biosensor shows a broad quantitative range, high sensitivity, and favorable specificity, avoiding complicated reporter elements and thermal cycling. The detection limit of the present biosensor is as low as 1.2 pg·mL^{-1} for CEA detection, which is mainly attributed to the cascade amplification strategy of the ERA and DNA walker. Moreover, this designed walker biosensor has been successfully applied to the detection of CEA in real serum samples. The present study expands the applications of DNA circuits in biological systems and facilitates the development of a new cascade amplification strategy for specific purposes.

ASSOCIATED CONTENT

Supporting Information

The Supporting Information is available free of charge on the ACS Publications website at DOI: 10.1021/acs.analchem.7b02073.

Calculation of the surface coverage of −COOH of the silica microspheres and the coupling efficiency of surface −COOH with the $-NH_2$ of H3, SEM and TEM characterizations of the silica microspheres, typical progress curve indicating two phases of the DNA machine operation, nondenaturing PAGE confirmation of the novel DNA machine based on a cascade amplification strategy of the ERA and DNA walker, optimizations of the assay conditions, sequences from 5′

Table 1. Determination of CEA in Real Human Serum Samples by Employing the Present DNA Machine

sample	data from hospital (ng·mL^{-1})	spiked (ng·mL^{-1})	found (ng·mL^{-1})[a]	recovery (%)	coefficient of variation (%)
		0	3.27 ± 0.13		6.1
1	3.39	4	7.23 ± 0.13	98	2.8
		10	12.95 ± 0.26	97	3.0
		0	5.55 ± 0.27		7.2
2	5.54	4	9.18 ± 0.22	96	3.5
		10	14.92 ± 0.77	96	7.6
		0	2.17 ± 0.11		7.8
3	2.23	4	6.12 ± 0.22	98	5.3
		10	11.93 ± 0.50	98	6.2
		0	4.38 ± 0.17		5.9
4	4.36	4	8.49 ± 0.34	101	6.0
		10	14.77 ± 0.39	103	3.9
		0	3.81 ± 0.16		6.3
5	3.67	4	7.76 ± 0.16	101	3.1
		10	13.81 ± 0.58	101	6.2
		0	20.25 ± 0.69		5.1
6	19.44	4	24.14 ± 0.88	103	5.4
		10	29.79 ± 0.89	101	4.5

[a]Average of 11 measurements.

DOI: 10.1021/acs.analchem.7b02073
Anal. Chem. 2017, 89, 9292−9298

to 3′-terminal of oligonucleotides used in this work, and comparisons of analytical performances of various methods for CEA assay (PDF)

AUTHOR INFORMATION

Corresponding Authors

*E-mail: yuyl@mail.neu.edu.cn. Phone: +86 24 83688944. Fax: +86 24 83676698.

*E-mail: jianhuajrz@mail.neu.edu.cn.

ORCID

Yong-Liang Yu: 0000-0001-9763-0954

Jian-Hua Wang: 0000-0003-2175-3610

Author Contributions

†M.-Q.H. and K.W. contributed equally to this work.

Notes

The authors declare no competing financial interest.

ACKNOWLEDGMENTS

This work is financially supported by the Natural Science Foundation of China (21475018 and 21235001) and the Fundamental Research Funds for the Central Universities (N160504010 and N141008001).

REFERENCES

(1) Chirieleison, S. M.; Allen, P. B.; Simpson, Z. B.; Ellington, A. D.; Chen, X. *Nat. Chem.* **2013**, *5*, 1000−1005.

(2) Li, B.; Ellington, A. D.; Chen, X. *Nucleic Acids Res.* **2011**, *39*, e110.

(3) Ge, L.; Wang, W.; Sun, X.; Hou, T.; Li, F. *Anal. Chem.* **2016**, *88*, 2212−2219.

(4) Yang, Y.; Huang, J.; Yang, X.; Quan, K.; Wang, H.; Ying, L.; Xie, N.; Ou, M.; Wang, K. *Anal. Chem.* **2016**, *88*, 5981−5987.

(5) Wang, K.; He, M.-Q.; Zhai, F.-H.; He, R.-H.; Yu, Y.-L. *Talanta* **2017**, *166*, 87−92.

(6) Tu, W.; Wang, W.; Lei, J.; Deng, S.; Ju, H. *Chem. Commun.* **2012**, *48*, 6535−6537.

(7) Fan, G.-C.; Zhu, H.; Du, D.; Zhang, J.-R.; Zhu, J.-J.; Lin, Y. *Anal. Chem.* **2016**, *88*, 3392−3399.

(8) Hou, L.; Tang, Y.; Xu, M.; Gao, Z.; Tang, D. *Anal. Chem.* **2014**, *86*, 8352−8358.

(9) Ren, K.; Wu, J.; Ju, H.; Yan, F. *Anal. Chem.* **2015**, *87*, 1694−1700.

(10) Li, L.; Wang, Q.; Feng, J.; Tong, L.; Tang, B. *Anal. Chem.* **2014**, *86*, 5101−5107.

(11) Li, J.; Zhong, X.; Zhang, H.; Le, X. C.; Zhu, J.-J. *Anal. Chem.* **2012**, *84*, 5170−5174.

(12) He, M.-Q.; Wang, K.; Wang, J.; Yu, Y.-L.; He, R.-H. *Anal. Bioanal. Chem.* **2017**, *409*, 1797−1803.

(13) Zong, C.; Wu, J.; Liu, M.; Yan, F.; Ju, H. *Chem. Sci.* **2015**, *6*, 2602−2607.

(14) Zong, C.; Wu, J.; Liu, M.; Yang, L.; Liu, L.; Yan, F.; Ju, H. *Anal. Chem.* **2014**, *86*, 5573−5578.

(15) Luo, C.; Tang, H.; Cheng, W.; Yan, L.; Zhang, D.; Ju, H.; Ding, S. *Biosens. Bioelectron.* **2013**, *48*, 132−137.

(16) Zuo, X.; Xia, F.; Xiao, Y.; Plaxco, K. W. *J. Am. Chem. Soc.* **2010**, *132*, 1816−1818.

(17) Chen, X.; Hong, C.-Y.; Lin, Y.-H.; Chen, J.-H.; Chen, G.-N.; Yang, H.-H. *Anal. Chem.* **2012**, *84*, 8277−8283.

(18) Chen, Y.; Xu, J.; Su, J.; Xiang, Y.; Yuan, R.; Chai, Y. *Anal. Chem.* **2012**, *84*, 7750−7755.

(19) Saiki, R. K.; Gelfand, D. H.; Stoffel, S.; Scharf, S. J.; Higuchi, R.; Horn, G.; Mullis, K.; Erlich, H. *Science* **1988**, *239*, 487−491.

(20) Duan, R.; Zuo, X.; Wang, S.; Quan, X.; Chen, D.; Chen, Z.; Jiang, L.; Fan, C.; Xia, F. *J. Am. Chem. Soc.* **2013**, *135*, 4604−4607.

(21) Wang, L.; Deng, R.; Li, J. *Chem. Sci.* **2015**, *6*, 6777−6782.

(22) Song, W.; Zhang, Q.; Sun, W. *Chem. Commun.* **2015**, *51*, 2392−2395.

(23) Ma, F.; Yang, Y.; Zhang, C.-Y. *Anal. Chem.* **2014**, *86*, 6006−6011.

(24) Zhou, H.; Liu, J.; Xu, J.-J.; Chen, H.-Y. *Chem. Commun.* **2011**, *47*, 8358−8360.

(25) Tao, C.; Yan, Y.; Xiang, H.; Zhu, D.; Cheng, W.; Ju, H.; Ding, S. *Chem. Commun.* **2015**, *51*, 4220−4222.

(26) Xu, Q.; Cao, A.; Zhang, L.-F.; Zhang, C.-Y. *Anal. Chem.* **2012**, *84*, 10845−10851.

(27) Liu, S.; Wang, C.; Zhang, C.; Wang, Y.; Tang, B. *Anal. Chem.* **2013**, *85*, 2282−2288.

(28) Heller, M. J. *Annu. Rev. Biomed. Eng.* **2002**, *4*, 129−153.

(29) McGlennen, R. C. *Clin. Chem.* **2001**, *47*, 393−402.

(30) Roh, Y. H.; Ruiz, R. C.; Peng, S.; Lee, J. B.; Luo, D. *Chem. Soc. Rev.* **2011**, *40*, 5730−5744.

(31) Zhang, F.; Nangreave, J.; Liu, Y.; Yan, H. *J. Am. Chem. Soc.* **2014**, *136*, 11198−11211.

(32) Yurke, B.; Turberfield, A. J.; Mills, A. P.; Simmel, F. C.; Neumann, J. L. *Nature* **2000**, *406*, 605−608.

(33) Yin, P.; Yan, H.; Daniell, X. G.; Turberfield, A. J.; Reif, J. H. *Angew. Chem., Int. Ed.* **2004**, *43*, 4906−4911.

(34) Cai, S.; Chen, M.; Liu, M.; He, W.; Liu, Z.; Wu, D.; Xia, Y.; Yang, H.; Chen, J. *Biosens. Bioelectron.* **2016**, *85*, 184−189.

(35) Chen, Y.; Xiang, Y.; Yuan, R.; Chai, Y. *Nanoscale* **2015**, *7*, 981−986.

(36) Li, W.; Wang, L.; Jiang, W. *Chem. Commun.* **2017**, *53*, 5527−5530.

(37) Mishra, R. K.; Hayat, A.; Mishra, G. K.; Catanante, G.; Sharma, V.; Marty, J.-L. *Talanta* **2017**, *165*, 436−441.

(38) Jung, C.; Allen, P.; Ellington, A. *Nat. Nanotechnol.* **2016**, *11*, 157−163.

(39) Guo, Y.; Chen, Q.; Qi, Y.; Xie, Y.; Qian, H.; Yao, W.; Pei, R. *Biosens. Bioelectron.* **2017**, *87*, 320−324.

(40) Tuerk, C.; Gold, L. *Science* **1990**, *249*, 505−510.

(41) Ellington, A. D.; Szostak, J. W. *Nature* **1990**, *346*, 818−822.

(42) Yang, J.; Dou, B.; Yuan, R.; Xiang, Y. *Anal. Chem.* **2016**, *88*, 8218−8223.

(43) Wang, S.; Zhang, Y.; Pang, G.; Zhang, Y.; Guo, S. *Anal. Chem.* **2017**, *89*, 1704−1709.

(44) Tomov, T. E.; Tsukanov, R.; Liber, M.; Masoud, R.; Plavner, N.; Nir, E. *J. Am. Chem. Soc.* **2013**, *135*, 11935−11941.

(45) Oh, S. S.; Plakos, K.; Lou, X.; Xiao, Y.; Soh, H. T. *Proc. Natl. Acad. Sci. U. S. A.* **2010**, *107*, 14053−14058.

(46) Rong, Z.; Wang, C.; Wang, J.; Wang, D.; Xiao, R.; Wang, S. *Biosens. Bioelectron.* **2016**, *84*, 15−21.

(47) Zong, C.; Wu, J.; Liu, M.; Yang, L.; Yan, F.; Ju, H. *Anal. Chem.* **2014**, *86*, 9939−9944.

(48) Ren, J.; Wang, J.; Han, L.; Wang, E.; Wang, J. *Chem. Commun.* **2011**, *47*, 10563−10565.

(49) Schaferling, M. *Wiley Interdiscip. Rev.-Nanomed. Nanobiotechnol.* **2016**, *8*, 378−413.

DOI: 10.1021/acs.analchem.7b02073
Anal. Chem. 2017, 89, 9292−9298